Sphalerite-wurtzite phase transformation in CdS

O. Zelaya-Angel[1,*] and R. Lozada-Morales[2]
[1]*Department of Physics, CINVESTAV-IPN, P.O. Box 14-740, Distrito Federal de México, Mexico 07360*
[2]*Posgrado en Optoelectronica, FCFM-BUAP, Puebla, 72570 Mexico*
(Received 28 July 2000)

An analytical study of the solid-solid phase transformation from the cubic zinc blende or sphalerite (S) metastable modification of CdS (β-CdS) to the wurtzite (W) hexagonal stable phase (α-CdS) is presented. Polycrystalline CdS layers in the cubic phase were prepared on glass substrates by means of chemical bath deposition. Films were heated in $Ar+S_2$ in the temperature (T) range 100–550 °C. X-ray diffraction data of annealed samples allowed us to observe a process of gradual change from β- to α-CdS. Optical absorption spectra let us obtain the band-gap energy (E_g) of samples (both as grown and annealed). The unit-cell volume (V) vs T line shape was explained as an interface movement of the S-W interdomain wall driven by T. The E_g vs T plot exhibits a minimum as a sharp peak at 300 °C, which is the T value assigned by us to the critical point (T_c) of the experimental structural transformation. The E_g vs V curve indicates an $E_g=AV^2+BV+C$ functional behavior. This E_g vs V dependence was explained through a relation between $(\partial E_g/\partial T)_P$ and C_P, where C_P is the specific heat at constant pressure. The C_P against T function was also calculated in the interval 300–800 K.

I. INTRODUCTION

Solid-state structural phase transitions have been widely investigated due to their important theoretical and applied implications. At present, there are many phenomena that remain open to suitable explanation, for instance, several actual mechanisms involved in the structural, optical, electrical, etc., properties during structural phase transitions in a large variety of solids such as superconductors, semiconductors, glasses, metalic alloys, among others. Abundant work has been reported on the cubic to hexagonal structural phase transition in crystalline semiconductors,[1–8] and some of them report, in particular, the sphalerite (S) to wurtzite (W) transformation in films[9–11] and nanometric clusters[12,13] of CdS. Phase transformations in semiconducting materials have been studied exhaustively theoretically and experimentally under application of either uniaxial or hydrostatic pressure;[2,9,14] however, the phase transformation caused by thermal annealing at normal pressures has not been completely understood up to now. In this paper we describe an insight into the structural transformation of semiconductors from a metastable modification to the stable crystalline phase in particular, into the old and well-known problem of the transformation of zinc blende or sphalerite CdS (β-CdS) to wurtzite CdS (α-CdS). The functional dependence of the unit-cell volume (V), the band-gap energy (E_g), and the specific heat at constant pressure (C_P) as functions of T, and the E_g vs V behavior are explained based upon the model of Akhiezer, Davidov, and Spol'nik[15] (model A) of phase transitions in crystals, and on the relationship between C_P and $(\partial E_g/\partial T)_P$ reported by Sirota.[16] Structural and optical characterizations were carried out at room temperature (RT), with the assumption that the crystalline state of annealed samples remains almost completely unalterable after cooling to RT. This approach phase transformation analysis might be useful for understanding phase change phenomena in a great variety of semiconductors and insulators.

II. EXPERIMENT

Polycrystalline thin films in the β-CdS phase were grown on glass substrates at 80 ± 1 °C by chemical bath deposition. The growth process has been described elsewhere.[17] Twenty-five samples of $5\times10\,mm^2$ in area were cut from the same growing lot. The thickness measured by profilometer was 200 ± 10 nm. The layers were simultaneously thermally annealed (TA) in an $Ar+S_2$ flux for 30 h at normal pressure in the T range 100–550 °C; afterward, samples were taken to RT. The stoichiometry of CdS measured by electron desorption spectroscopy was $[Cd]/[S]\sim1.0$ within 3% in as-grown (AG) and annealed films. X-ray diffraction (XRD) data were obtained by means of a Siemens D5000 diffractometer, and the optical absorption (OA) spectra, in the UV-visible spectral region, were measured using a Unicam spectrophotometer. All these characterization measurements were carried out at RT. The XRD information allowed us to calculate the interplanar distance (δ) of the lattice and the unit-cell volume (V). δ refers to (111) and (002) planes for the S and W lattices, respectively. The determination of E_g values was carried out using the formula $(\alpha h\nu)^2=(cte)(h\nu+E_g)$ of direct electronic transitions, where α is the OA coefficient. In the $(\alpha h\nu)^2$ vs $h\nu$ plot, the intersection of the extrapolated straight part of the curve with the energy axis equals E_g, as illustrated in Fig. 1.

III. RESULTS AND DISCUSSION

XRD patterns of CdS layers show the evolution from β- to α-CdS as the diffractograms progress from the AG sample to the 550 °C TA sample, as reported in previous work.[18] The [111] direction in crystalline β-CdS coincides with the [002] direction of crystalline α-CdS after structural transformation. Figure 2 displays $\delta(T)$ as a function of T. The line shape can be divided into three regions. In the first region, in the range 80–225 °C, δ exhibits large oscillations whose am-

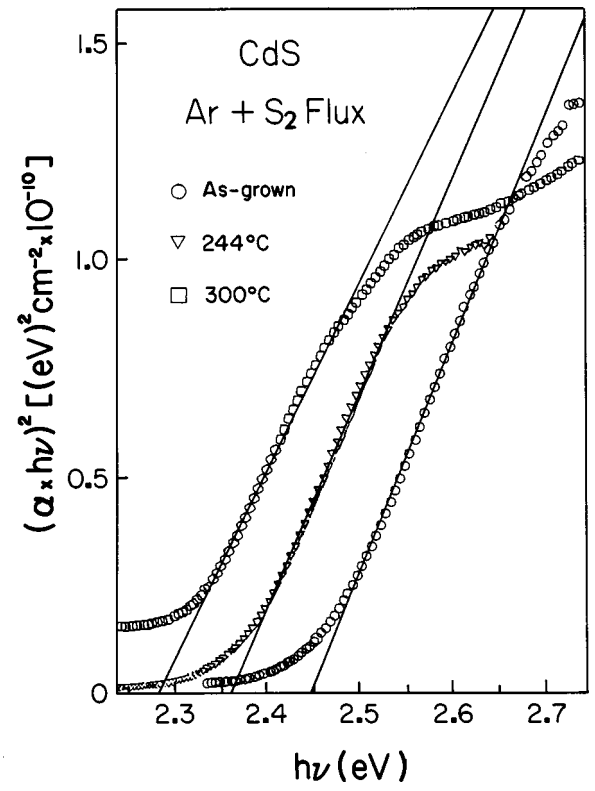

FIG. 1. $(\alpha h\nu)^2$ vs the photon energy $(h\nu)$ plot for as-grown and two annealed samples. The extrapolation of the straight line to the $h\nu$ axis gives E_g.

plitude shows a slow decrease as T goes toward 225 °C. The second region, $225 \leqslant T \leqslant 350$ °C, is characterized by an approximately linear dependence of δ vs T. The last region, 350–550 °C, also displays oscillations, but smaller than in the first region. Here, the amplitude of δ damps rapidly, becoming flat from $T \cong 470$ °C onward. The final value $\delta = 3.3550 \pm 0.0001$ Å is shorter than the reported value for bulk W-CdS. $\delta = 3.3599$ Å. This shift in the final δ value might be due to the polycrystalline character of the CdS thin films and the amorphous nature of the substrate. The inset at the top of Fig. 2 illustrates the unit-cell (UC) volume V plotted against T, calculated by using the (hkl) indices of peaks displayed in the diffractograms. Since theoretically $V(S) = 2V(W)$, twice the real UC volume of W-structured samples was employed in the V vs T plot, to have the same numerical order of V for comparison. This functional dependence, with a symmetric point at $T = 300$ °C, the critical temperature (T_c) of the phase transition, was reported by us in recent work.[19] Actually, taking into account that the pressure was maintained constant (normal pressure) during the annealing process, the relation[19]

$$V = (2.65 \tanh\{[(1.89 \times 10^{-2})\,\mathrm{K}^{-1}](T - 573)\} + 194.65\,\mathrm{K}^{-1}) \quad (1)$$

can be considered as the equation of state of the UC of the material during the phase transformation. In this relation, according to the model A, V represents the growing volume of the new phase, which starts from point nucleation centers, followed by an interface movement (the intermixed S-W wall) driven by a thermally activated process. In theory, S and W crystalline phases have the same mass density value, so that no volume change would be expected during the structural transformation. In practice, in tetracoordinated lattices of binary compounds, in the S structure the four AB distances of the AB_4 tetrahedron necessarily have equal lengths, but in the W structure the AB length parallel to the c axis is either longer or shorter than the other three.[20] If all or most of the neighboring coordination polyhedra show an equidirectional deformation, crystallites of the hexagonal phase will growth, if deformation implies an increase of the c axis.[20] In our case, the AB length parallel to the c axis is longer than the other three AB distances in all the layers, from the 300 °C TA sample onward. For annealing temperatures below 300 °C, only samples with the S structure are observed in XRD diffractograms, with the four AB lengths increasing equally with T. Despite the presence of the S phase alone, the A model[15] predicts the presence of W-structured regions for annealing temperatures below 300 °C, whether by generation of W nucleation centers or by

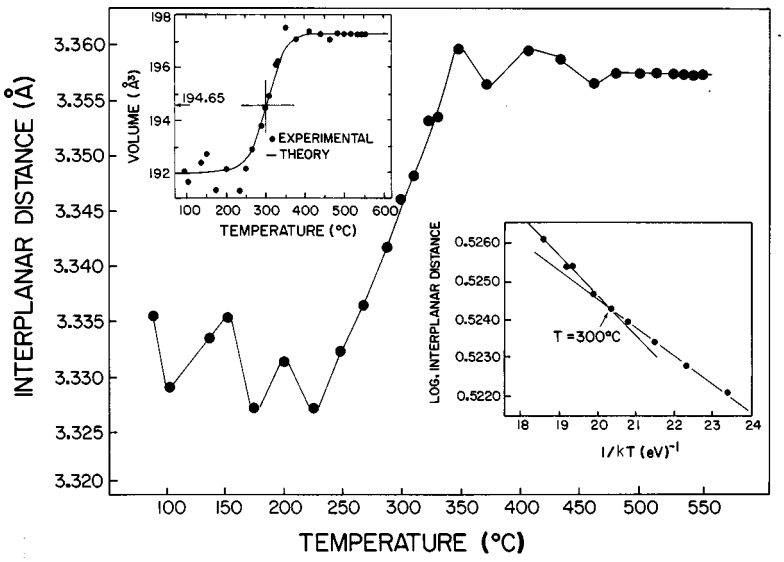

FIG. 2. Interplanar distance δ as a function of annealing temperature. The top inset shows the unit-cell volume plotted against the annealing temperature. The bottom inset illustrates the logarithm (base 10) of the interplanar distance vs the inverse annealing temperature.

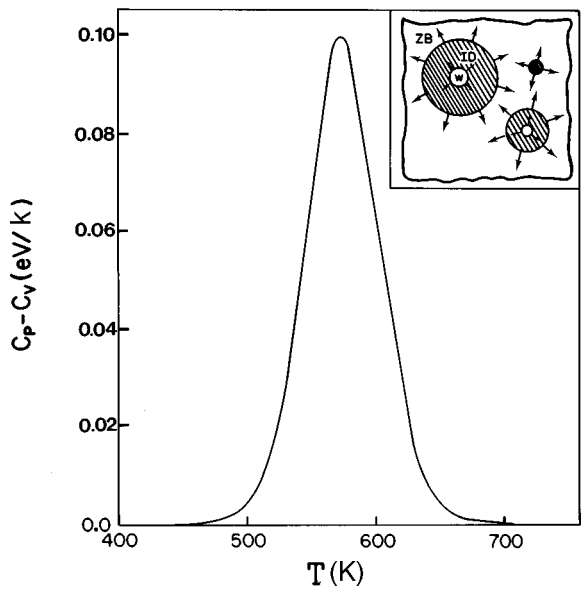

FIG. 3. The difference of specific heats C_P-C_V as a function of annealing temperature. The inset represents schematically a cubic [*S* or zinc blende (ZB)] CdS crystalline grain with *S*-*W* interdomains (ID) and *W*-structured regions growing inside the volume of ZB structure.

considering the small *W* regions already present in AG samples, both increasing with *T*. The more probable explanation for the lack of observation of the *W* phase is the existence of a preferred growth orientation of the *W* phase along the [002] direction, which is parallel to the [111] direction of the dominant *S* phase. With this in mind, it is correct to expect no presence of peaks belonging to the *W* phase, in addition to (002), in the XRD diffractograms for annealing temperatures below 300 °C. As a matter of fact, this peak overlaps almost completely the (111) peak of the *S* phase. The *W* structure does not form a sharp border with the rest of the *S* structure in each grain, there is a mixture of both phases in a well-defined interdomain wall, whose width grows with *T*. Furthermore, taking into account that the width of *S*-*W* interdomain walls reaches up to 9–16 % of the average grain size of the films,[19] different nucleation centers of the *W* phase grow volumetrically inside each grain as *T* goes to higher values, and the external borders of these interdomain walls contact each other until $T\sim 300$ °C, with an effective internal volume of regions with *W* structure extremely small as compared with the total volume of the crystallite (see inset in Fig. 3). If this is the case, the effect of a detectable (by XRD) total volume of *W*-structured lattice can be neglected for $T\leqslant 300$ °C.

In the first region (80–225 °C), we think that the large oscillations in δ are due to arrangement of vacancies ($\mathcal{V}$) and interstitials ($\mathcal{I}$) of cadmium as *T* increases. An important density of $\mathcal{V}$-$\mathcal{I}$ Cd pairs is created during the growth process;[21] more $\mathcal{V}$-$\mathcal{I}$ Cd pairs, or Frenkel defects, originate during the TA of layers because of the movement of Cd cations surmounting an energy barrier in order to produce the structural phase change.[21,22] As a matter of fact, the *S*-*W* interdomain contains plenty of $\mathcal{V}$-$\mathcal{I}$ Cd pairs.[19,21,22] These $\mathcal{V}$-$\mathcal{I}$ pairs are also being created at random at different points inside the grain volume, due to thermal nucleation centers. Our opinion is that formation of $\mathcal{V}$ clusters and localized $\mathcal{I}$ concentrations causes fluctuations in the lattice volume since the driving thermal power sometimes either joins or spreads out these aggregates of defects, and it also annihilates $\mathcal{V}$-$\mathcal{I}$ pairs. For $T\geqslant 225$ °C, the organized movement of $\mathcal{V}$-$\mathcal{I}$ pairs predominates to induce the structural phase change. From here, the phase transformation process runs faster by reducing the volume of the *S*-*W* walls and, consequently, increasing the fraction of *W*-structured lattice. In the last region, $\mathcal{V}$-$\mathcal{I}$ Cd pairs gradually disappear and *V* fluctuations are rapidly annulled. The inset at the bottom of Fig. 2 displays the logarithm of δ expansion versus the inverse *T* in the second interval of TA (225–350 °C). This volume expansion is two orders of magnitude larger than the normal thermal volume expansion due to the enlargement of vibrational amplitude of ions in the lattice when *T* increases. Moreover, the normal thermal expansion in CdS is not an exponential thermally activated phenomenon, but linear with *T*. The graph evidences a change in slope just at $T=300$ °C, the temperature value that we have associated with the critical point (T_c) of the transition.[18,19,21] The discontinuity in the activation energy at $T=300$ °C can be identified with different energy barriers when the crystallite structure passes from an *S*-dominated to a *W*-dominated lattice. The inset in Fig. 3 is a schematic illustration of the phase transformation process through interdomain and *W*-region growth. The heat capacity must change during the structural transformation because of the generation of a larger density of states. With the purpose of observing the change, $C_P(T)$ was determined from the relation $C_P-C_V=\alpha^2\beta^{-1}VT$, where α is the volume thermal expansion coefficient $[V^{-1}(\partial V/\partial T)_P]$ and β the compressibility coefficient $[-V^{-1}(\partial V/\partial P)_T]$. $V^{-1}(\partial V/\partial T)_P$ can be deduced from $V(T)$ defined by Eq. (1). It should be noticed that $\alpha(T)$ results in a continuous function. C_P-C_V can be a discontinuous function only if $\beta(T)$ is discontinuous during the phase transformation. $\Delta V/V$ is discontinuous when CdS undergoes a phase transformation from the wurtzite to rocksalt structure under pressure; nevertheless, before reaching the rocksalt structure, CdS first must pass through the metastable *S* phase,[9] and no discontinuity was observed.[23] It is expected that CdS, in this experiment, has a similar continuous behavior in $\Delta V/V$ to that observed in ZnS, when its lattice transforms from *S* to *W* under pressure.[23] In general, $\beta(T)$ has a slow dependence on *T*,[24(a)] which we took advantage of to use a constant value in calculations. The first derivative of Eq. (1) allows one to obtain the function

$$C_P-C_V=\frac{(3.48\times 10^{-2})T\,\mathrm{sech}^4\{[(1.89\times 10^{-2})\,\mathrm{K}^{-1}](T-573\,\mathrm{K})\}}{2.65\tanh\{[(1.89\times 10^{-2})\,\mathrm{K}^{-1}](T-573\,\mathrm{K})\}+194.65}\ \mathrm{eV/K\ molec.} \quad (2)$$

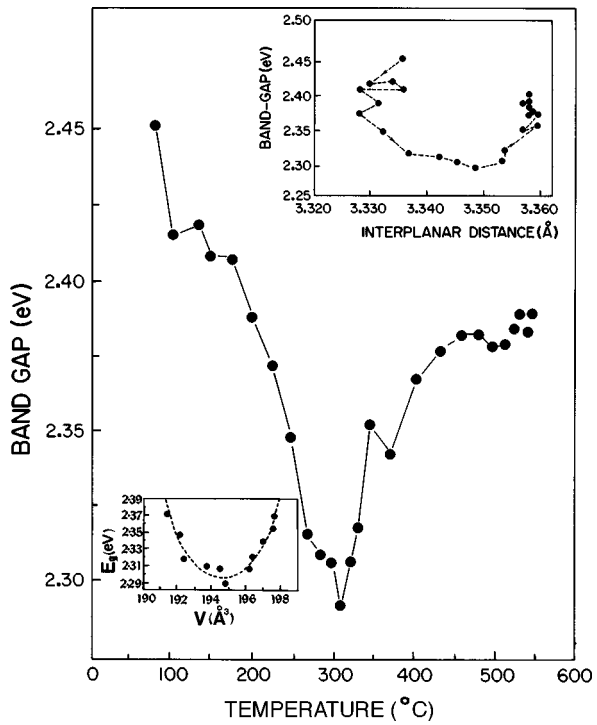

FIG. 4. Band-gap energy as a function of annealing temperature. The top inset shows that Vegard's law is not valid. The bottom inset displays the band gap vs unit-cell volume plot. The band-gap energy shows a parabolic dependence on the unit-cell volume. Dashed line is the least-squares minima calculation.

In the 3.48×10^{-2} factor are included an average compressibility coefficient from two values reported[23,25] ($\beta=2.23\times10^{6}\,\mathrm{bar}^{-1}$) and the fact that the unit-cell volumes considered here have four molecules of CdS. Figure 3 depicts the C_P-C_V versus T function in the interval 450–700 K. This curve peaks at 573 K, the critical point T_c of the structural transformation. The form of the curve clearly indicates a phase transition between two different crystalline structures of the material. As this curve is continuous through T_c, which implies that α and β are also continuous, the transition is of the first order.[24(b)] Obviously, the transformation from *S*- to *W*-CdS is a gradual process without any abrupt step in the C_P-C_V functional dependence on *T*. It must be noted that C_V cannot have any abrupt change, at least at the high temperatures used here. The order-disorder transformation is not first order, even though Yu and Gielisse[9] suggest that $S\rightarrow W$ is an order-disorder transformation that can be considered analogous to a first-order transformation, because the material transforms in a series of infinitesimal steps from one ''phase'' to the next one as the free-energy curve of each successive ''phase'' becomes the lowest.

The E_g vs T dependence is depicted in Fig. 4. The difference between $E_g=2.45$ eV for AG cubic CdS film and the standard value 2.40 eV for α-CdS bulk is within the well-known accepted difference (0.1 eV).[26] Figure 4 clearly evidences a minimum value $E_g=2.29$ eV, which peaks sharply at T_c (300 °C=573 K). For $T>300$ °C, E_g turns back to higher energies, although it does not reach its initial value but stabilizes at 2.38 eV. The E_g evolution with T in the range 80–225 °C is less affected than δ and V in the same T range. Probably, δ and V fluctuations are well localized in the *W-S* interdomain; however, these fluctuations alter the total volume of each crystallite. In contrast, the E_g measurement is a result of light signals coming from the whole bulk of grains, in which are zones having neither clusters nor aggregates of defects, but mostly well-structured material. Above T_c, in agreement with Vegard's law, one expects the E_g value to follow the same trend toward lower energies, because δ continues increasing, but it does the opposite. For $T>T_c$ the binding forces of the *W* lattice overcome the volume increase effects. E_g peaks acutely at T_c due to the fact that there exists a dV/dT maximum value, after which the ever-increasing density of larger *AB* lengths starts to have a slower growth rate and stops at saturation ($T>500$ °C). It is worth while remarking that disorder is not the origin of the sharp minimum in the E_g plot, since the calculation of E_g values is based on the parabolic band structure around the Γ point of the UC, i.e., using the well-known relation $(\alpha h\nu)=(cte)(h\nu+E_g)$. Here, E_g is the intercept of the straight line with the $h\nu$ axis, as demonstrated in Fig. 1. This means that the band structure either swells or shrinks according to whether the UC volume diminishes or increases.

The upper inset of Fig. 4 shows E_g as a function of δ. Obviously, Vegard's law is not valid along the entire range swept by δ; nevertheless, in a small range near $\delta=3.345$ Å, corresponding to T_c, the experimental points resemble a linear dependence of E_g on δ. In the inset at the bottom of Fig. 4, the E_g vs V data plot exhibits a parabolic dependence, through a set of well-scattered experimental points in the V range of, approximately, the linear part of the V vs T line (in the interval 225–350 °C of the top inset of Fig. 2). The scattering of experimental points in the E_g vs V plot around the parabolic fitting is larger than the error in direct E_g measurements added to the error produced by calculating the E_g error propagation from V and T error bars produced in their individual measurements. The dispersive character of the points is mainly due to intrinsic fluctuations of E_g and V. By means of least-square minima applied to those experimental measurements, one can obtain the phenomenological expression

$$E_g=\{[(1.05\pm0.34)\times10^{-2}\,\text{Å}^{-6}]V^2-(4.08\pm1.32)\,\text{Å}^{-3}\times V+(400\pm127)\}\,\text{eV}. \tag{3}$$

For a theoretical fitting of this function, the relation

$$C_P=-A(\partial E_g/\partial T)_P \tag{4}$$

proposed by Sirota[16] can be used. A is a constant parameter depending on the specific semiconductor studied. An equivalent relation,

$$E_g=-A^{-1}\int_{T_0}^{T}C_P\,dT \tag{5}$$

was employed by us. The integration of Eq. (2) from T_0 to any T value near T_0 can be approximated by using in Eq. (2) $\operatorname{sech}x\approx1$ and $\tanh x\approx x$, for $x\rightarrow0$, in our case when $T\rightarrow T_0$. In this way,

$$\int_{T_0}^{T}(C_P-C_V)dT \cong (3.48\times10^{-2}) \times \int_{T_0}^{T}\frac{T\,dT}{(5.0\times10^{-2})(T-T_0)+194.65}. \quad (6)$$

The integration process supplies

$$\int (C_P-C_V)dT = (2.06\times10^{-2}\{52.9(T-573)-(1.75\times10^{5}) \times \ln[1+(2.57\times10^{-4})T]\})\ \text{eV/K molec.}$$

Afterward, one can use the series $\ln(1+x)=x-\frac{1}{2}x^2+\frac{1}{3}x^3-\cdots$. Up to second order in the series, the following expression is reached: $\int C_P dT=\{(7.48\times10^{-5})T^2+(1.48\times10^{-2})T-55.21+\int C_V dT\}$ eV/molec. Employing the Debye temperature of CdS, it can be shown that the variation of C_V from 450 to 700 °K is $0.983(3R)$ to $0.992(3R)$, respectively, where $R=8.314$ J/K molec.$=8.62\times10^{-5}$ eV/K molec., is the molar constant of gases. In this case, C_V can be taken constant in this temperature range (average $C_V=2.55\times10^{-4}$ eV/K mol). Then $\int C_V dT=[(2.55\times10^{-4})T-0.146]$ eV/molec. Consequently,

$$\int_{573\,\mathrm{K}}^{T} C_P dT=\{(7.48\times10^{-5})T^2-(1.51\times10^{-3})T-55.36\}\ \text{eV/molec.} \quad (7)$$

In order to get E_g as a function of V, we used the V vs T experimental dependence in the same range of the E_g parabolic dependence, i.e., the interval of V from 191 to 198 Å[8] (bottom inset of Fig. 4). In this region Eq. (1) can be approximated to the linear function $V=(2.65\{[(1.89\times10^{-2})\,\mathrm{K}^{-1}](T-573)+194.65\})\,\text{Å}^3$, equivalent to $T=[(20.0\,\text{Å}^3)V-4466]$ K. In this way, by replacing this last expression in Eq. (7), one obtains

$$\int_{573\,\mathrm{K}}^{T} C_P dT=\{(2.99\times10^{-2})V^2-13.06V+489\}\ \text{eV/molec.} \quad (8)$$

The constant A in Eq. (4) should be evaluated from experimental data already reported. Thus, $(\partial E_g/\partial T)=-3.90\times10^{-4}$ eV/K (average),[27(a)] and $C_P=13.1$ cal/K mol$=2.8\times10^{-4}$ eV/K molec. (average).[27(b)] Both values, $\partial E_g/\partial T$ and C_P, were taken at room temperature. The constant of Eq. (3) was evaluated utilizing both these data, obtaining $A'=-0.71$ molec.$^{-1}$. In Eq. (8) the volume V is that of the UC, which has four CdS molecules. According to this, $A=4A'=-2.84$ molec.$^{-1}$. Then Eq. (5), $E_g=-A^{-1}\int C_P(V)dV$ results in

$$E_g=\{[(1.05\pm0.15)\times10^{-2}\ \text{Å}^{-6}]V^2-[(4.60\pm0.35)\ \text{Å}^{-3}]V+(482\pm40)\}\ \text{eV}. \quad (9)$$

Within the error bars, generated in Eq. (9) partially because of averaging of the β, C_P, and $\partial E_g/\partial T$ data reported, and partially from the V vs T dispersion error in the experiment observed in the upper inset of Fig. 2 and in the approximated integration, this is, in principle, a coincident expression with the phenomenological relation of Eq. (2), and explains clearly the E_g vs V dependence in the phase transformation. In fact, disorder in the lattice does not exert an important influence in the phase transformation. Figure 1 shows a longer tail at low energies in the OA data of the 300 °C TA sample, evidencing that there is a maximum disorder in the lattice, which does not affect the E_g calculation. This means that E_g vs V behavior is caused in essence, by the V vs T dependence, in agreement with the model of Akhiezer, Davidov, and Spol'nik, in the *S-W* phase transition of CdS. The work done by the system against the atmospheric pressure is $\sim4\times10^{-3}$ eV, which can be considered negligible. Since the performance of the calculated $C_P(T)$ function through the critical point predicts the E_g vs V dependence and no discontinuity is necessary, the *S-W* transition can be assumed to be first order.

IV. CONCLUSION

In summary, we have completely described the phase transition process of CdS thin films from sphalerite to wurtzite structural phases, at normal constant pressure, based on x-ray diffraction and optical absorption measurements. The experimental results were theoretically explained by using a phase transition model and the $C_P=-A(\partial E_g/\partial T)_P$ functional dependence.

ACKNOWLEDGMENTS

The authors are grateful to Dr. Y. Gurevich for a critical reading of the work, to Dr. D. O'Connors for a review of the manuscript, and to Ing M. Guerrero for her technical assistance. This work was partially supported by CONACyT, Mexico.

*Corresponding author. FAX: (52-5)747 7096; Email address: ozelaya@fis.cinvestav.mx

[1] J. L. Birman, Phys. Rev. **115**, 1493 (1959).
[2] E. Rapaport and C. W. T. F. Pistorious, Phys. Rev. **172**, 838 (1968).
[3] C. Yeh, Z. W. Lu, S. Froyen, and A. Zunger, Phys. Rev. B **45**, 12 130 (1992).
[4] R. G. Pearson, J. Mol. Struct. **260**, 11 (1992).
[5] K. Karch and F. Bechsted, Phys. Rev. B **56**, 7404 (1997).
[6] Y. Q. Zhu, T. Sekine, T. Kobayashi, and E. Takazawa, J. Mater. Sci. **33**, 5883 (1998).
[7] M. I. Eremets, K. Takemura, H. Yusa, D. Goldberg, Y. Bando, V. D. Blank, Y. Sato, and K. Watanabe, Phys. Rev. B **57**, 5655 (1998).
[8] U. Starke, J. Schardt, J. Benhart, M. Franke, and K. Heinz, Phys. Rev. Lett. **82**, 2107 (1999).
[9] W. C. Yu and P. J. Gielisse, Mater. Res. Bull. **6**, 261 (1971).
[10] Ph. Hoffmann, K. Horn, A. M. Bradshaw, R. L. Johnson, D. Fuchs, and M. Cardona, Phys. Rev. B **47**, 1639 (1993).
[11] D. Lincot, B. Mokili, M. Froment, R. Cortés, M. C. Bernard, C.

Witz, and J. Lafait, J. Phys. Chem. B **101**, 2174 (1997).
[12] M. B. R. Krishna and R. A. Friesner, J. Chem. Phys. **95**, 8309 (1991).
[13] W. Vogel, J. Urban, M. Kundu, and S. Kulkarni, Langmuir **13**, 827 (1997).
[14] M. Haase and A. P. Alivisatos, J. Phys. Chem. **96**, 6756 (1992).
[15] I. A. Akhiezer, L. N. Davidov, and Z. A. Spol'nik, Fiz. Tverd. Tela (Leningrad) **24**, 2314 (1982) [Sov. Phys. Solid State **24**, 1313 (1982)].
[16] N. N. Sirota, in *Chemical Bond in Semiconductors and Thermodynamics*, edited by N. N. Sirota (Consultants Bureau, New York, 1968), p. 7.
[17] J. L. Martínez, G. Martínez, G. Torres-Delgado, O. Guzmán, O. Zelaya-Angel, and R. Lozada-Morales, J. Mater. Sci.: Mater. Electron. **8**, 399 (1997).
[18] O. Zelaya-Angel, J. J. Alvarado-Gil, R. Lozada-Morales, H. Vargas, and A. Ferreira Silva, Appl. Phys. Lett. **64**, 291 (1994).
[19] O. Zelaya-Angel, H. Yee-Madeira, and R. Lozada-Morales, Phase Transit. **70**, 11 (1998).
[20] L. Daweritz, J. Cryst. Growth **23**, 307 (1974).
[21] R. Lozada-Morales and O. Zelaya-Angel, Thin Solid Films **281-282**, 386 (1996).
[22] G. Burley, J. Phys. Chem. **68**, 1111 (1964).
[23] C. F. Kline and D. R. Stephens, J. Appl. Phys. **36**, 2869 (1965).
[24] R. A. Swalin, *Thermodynamics of Solids*, 2nd ed. (Wiley, New York, 1972), (a) p. 31; (b) p. 90.
[25] G. A. Samara and A. A. Giardini, Phys. Rev. **140**, A388 (1965).
[26] M. Cardona, M. Weinstein, and G. A. Wolff, Phys. Rev. **140**, A633 (1965).
[27] I. Broser, R. Broser, and M. Rosenzweig, in *Numerical Data and Functional Relationships in Science and Technology*, edited by O. Madelung, M. Schutz, and H. Weiss, Landolt-Börstein, New Series, Group III, Vol. 17, Pt. b (Springer-Verlag, Berlin, 1982), (a) p. 167; (b) p. 193.